Baltimore, Maryland
NOISE-CON 2004
2004 July 12-14

Measurements of Acoustic Properties of Porous and Granular Materials and Application to Vibration Control

Junhong Park[1], Daniel L. Palumbo[2], National Research Council[1], Structural Acoustics Branch[2], NASA Langley Research Center, Hampton, Virginia 23681-2199,

For application of porous and granular materials to vibro-acoustic controls, a finite dynamic strength of the solid component (frame) is an important design factor. The primary goal of this study was to investigate structural vibration damping through this frame wave propagation for various poroelastic materials. A measurement method to investigate the vibration characteristics of the frame was proposed. The measured properties were found to follow closely the characteristics of the viscoelastic materials - the dynamic modulus increased with frequency and the degree of the frequency dependence was determined by its loss factor. The dynamic stiffness of hollow cylindrical beams containing porous and granular materials as damping treatment was measured also. The data were used to extract the damping materials' characteristics using the Rayleigh-Ritz method. The results suggested that the acoustic-structure interaction between the frame and the structure enhances the dissipation of the vibration energy significantly.

1. INTRODUCTION

As advanced structural elements such as honeycomb panels are increasingly used in vehicles, total mass of the structure continues to decrease, especially in aerospace applications [1]. The decrease in airframe mass can result in increased cabin noise. To maintain interior noise levels, either existing treatment must be supplemented (adding mass) or more efficient treatment must be developed. Structural vibration damping contributes to the minimization of these noise-related problems. Porous and granular materials have been widely used to vibration damping and noise-control applications. Two separate dilatational waves can propagate through the fluid and the solid component (frame) in porous materials. [2] They are referred to here as airborne and frame waves, respectively, [3] for noise-control materials where the fluid is air. To investigate and measure the acoustic properties of porous materials, it is often considered that the frame of the porous materials is rigid or limp. In the case of the airborne wave propagation only, it is possible to measure the acoustic properties through several different methods (see Ref. 4 for a review of these method and the transfer-matrix method). The measurement of the vibration characteristics of the frame under time-varying external loads [5-6] received less attention compared to those through air. However these properties are important design factors that determine the acoustic properties of the material when the elasticity of the frame is considerably large. [3] Also, for fiberglass and granular materials where the frame vibration is often assumed to be limp or rigid, [4, 7-9] the actual measurements of the vibration characteristics of the frame are essential if sound transmission characteristics are to be understood and compared.

The absorption and dissipation through frame and airborne waves in acoustic treatment contribute significantly to vibration damping of the underlying structure which, in turn, increases the sound transmission loss. As an example, consider multi-panel structures lined with porous materials. [3] Cummings et al. [10] investigated the damping of plate vibration using acoustic foams. By placing the acoustic foam close to the vibrating plate, the damping ratio in the plate was increased significantly. Their analysis showed that the absorption and succeeding dissipation of the sound radiation from the plate through airborne wave propagation in the foam increased the damping of structural waves of the plate. The damping of structural vibration using granular materials has been a research subject for decades. It has been shown that the conduction of energy into the granular material and the subsequent dissipation [11-15] raise the vibration damping significantly. It has been suggested that the maximum loss factor occurs at quarter wavelength resonances inside the granular material. [12, 13] Using a statistical energy analysis, Sun et al. [14] measured the damping ratio of structures containing sand as a damping treatment and showed that maximum damping occurred at frequencies where the thickness of the sand approaches 0.05 λ ($\lambda=c/f$). This suggests that the maximum damping frequency is lower than the quarter or half

wavelength resonance, i.e., the frequencies at which the thickness of the sand is 0.25 λ or 0.5 λ, respectively. This discrepancy may be due to the assumed wave speed in the sand of 150 m/s [12-14] which is rather higher than those measured for the material in this study. Using a wave propagation approach, McDaniel et al. measured vibration damping in beams treated with elastomeric beads. [15] The loss factor of the beam bending stiffness was found to vary strongly with frequency when the polymeric beads were known to be dissipating vibration energy.

In this study, an experimental method is proposed in which the dynamic characteristics of porous and granular materials, especially those of the frame, are measured. Under controlled longitudinal vibration, the transfer function between the excitation and the response is measured. The experimental setup is designed so that the effects of airborne waves have negligible impact on the measurements. The wave propagation characteristics – wave speeds and their loss factors, are obtained from the measured transfer function. The measured characteristics are analyzed using the linear viscoelastic theory. The impact of several parameters, such as vibration amplitudes, static loading, and particle size, on the measured dynamic properties are investigated.

The structural vibration damping resulting from the application of porous and granular materials is considered as a noise control treatment. The dynamic bending stiffness of hollow cylindrical beams containing different damping materials is investigated. The Rayleigh-Ritz method is used to predict the beam response and the frequency dependent variation of the bending stiffness loss factor after having taken into account the acoustic-structure interactions. The predictions are compared to the experimental results obtained from the transfer function methods and the vibration measurements of the cylindrical beams. From this comparison, the mechanism of damping of the structural vibration through the porous and granular materials is analyzed.

2. MEASUREMENTS OF VIBRATION CHARACTERISTICS OF THE FRAME OF POROUS AND GRANULAR MATERIALS

In the analysis of wave propagation through granular material, it is often assumed that the particles are limp, i.e., frame wave speeds are close to zero. For airborne wave propagation, the wave speed ranges from 100-300 m/s, and it depends on the mechanical properties of the particles, especially diameter (the airborne wave speed increased with increasing particle diameter). In the case where the granular material is applied as a damping treatment, or to minimize sound transmission through the structure, the frame wave will contribute significantly due to the large density of the solid component.

For small amplitude harmonic vibration, complex elastic moduli are used to take into account the dissipation of vibration energy. For uniaxial vibrations the complex modulus is defined as,

$$\hat{E}(\omega) = E(\omega)[1 + i\eta_E(\omega)], \tag{1}$$

where E is the dynamic moduli, $i = \sqrt{-1}$, and η_E is the loss factor of the complex modulus. To measure these dynamic properties using the transfer function method, controlled excitation and precisely known boundary conditions are required. The longitudinal vibrations of rod-like specimens are widely used to measure dynamic properties of polymers [16-18]. However, it is difficult to induce a controlled vibration in granular material formed into a rod since it will collapse. If a container, such as a tube is used to hold the specimen in the shape of the rod, the friction between the granular material and the container has significant impacts on the vibration characteristics. [11] To minimize this friction related problem, the longitudinal vibration is induced in the material specimen as shown in Figure 1. The lateral dimensions of the specimen in the y and z directions are much larger than the thickness of the specimen, h. The airborne waves freely propagate through the attached mass. This setup has several advantages. Since the airborne wave speeds are typically larger than those of the frame wave, longitudinal vibration of the specimen of small thickness (measured in the direction of the induced vibration) is preferred to prevent the resonance of the acoustic waves in the frequency range of interest. Consequently, standing wave resonances observed in the measured transfer function are due mostly from the vibration of the frame since the first natural frequency of the frame is much smaller than that of the airborne wave. Also, the frame response is not too small or too large compared to airborne wave propagation if the thickness is as small as possible. This minimizes the effects of couplings between acoustic waves and frame waves as taken into account in many poroelastic wave propagation theories. In addition, the effects of the resonance in the width can be neglected compared to those in the thickness (x-direction). The strain in the y and z directions is assumed to be negligibly small under the longitudinal vibration. Under these conditions, the vibration analysis of the granular media can be reduced to two dimensions. This configuration is also suitable for measuring the frame dynamic characteristics of fiberglass and acoustic open cell foams which the acoustic wave propagation has significant impacts on the frame vibrations.

In Figure 1, the longitudinal vibration response of the specimen is measured at the attached mass. This attached mass prevents the shear or bending vibration of the specimen, so that it is only under longitudinal vibration. Therefore, the mass should be rigid in the frequency range of interest to minimize the effects of its dynamics, such as from the transverse bending vibration. However, the mass should be as small as possible to minimize the initial static compression of the specimen due to the mass loading, especially when specimens of small elasticity are tested, for example, lightweight microspheres and fiberglass. Also, airborne waves should be able to freely propagate through the attached mass so that the mass responds only to the vibration of the frame. Figure 2 shows a schematic of the experimental setup used for the test. Nomex honeycomb was used to satisfy the requirements for the attached mass. The honeycomb had a cross-sectional dimension, thickness, and mass of 5.1x5.1 cm^2, 1.9 cm, and 3.6 g, respectively. Each honeycomb cell dimension was 0.32 cm, providing free propagation of the acoustic wave through the honeycomb in the x-direction. The cell was small enough so that the honeycomb appeared to the particles as a rigid plate and prevented bending and shear vibration of the specimen. The first natural frequency of the honeycomb under free-free boundary conditions was 880 Hz, which suggested that its dynamics were negligible and could be regarded as a rigid mass within frequency range of interest.

The edges of the granular specimens were terminated by corrugated acoustic foam to minimize the resonance in the y and z directions. The acoustic foam border was required to hold the granular material in place. Except for the absorption and dissipation of the standing waves in the y and z directions, the corrugated acoustic foams should have no significant effect on the dynamics of the longitudinal vibration of the specimen. Under this setup, the lateral strain is negligibly small. The wave propagation in the porous material can be analyzed through the Biot theory [2,3] that takes both of the frame and airborne wave propagation and their interaction into accounts. When the thickness is small and the attached mass responds only to the frame of the material, the equation of motion simplifies to those of the classical rod theory. The measurement procedure based on the longitudinal vibration of the specimen is well established. [16-18] From the measured wavenumber in the solid, the dynamic stiffness, $\hat{B}$, and the wave speed, $\hat{c}$, are obtained. In the transfer function method, a standing wave is analyzed to estimate the wavenumber from the measured transfer functions. For longitudinal vibration as shown in Figure 1, the measured transfer function between the input and output displacements is related to the wavenumber through

$$\hat{w}(x=h)/w_0 = \left(\cos\hat{k}h - (m/m_s)\hat{k}h\sin\hat{k}h\right)^{-1} \tag{2}$$

where $m_s=\rho Ah$ is the mass of the specimen, A is the cross-section and m is the mass of the attached mass. The Newton-Rapson method is used to obtain the complex wavenumber from equation (2) and the measured transfer function after separating the real and imaginary parts. There are infinitely many solutions that satisfy equation (2). Among the possible solutions, only one is physically acceptable. The physically acceptable solution for the wavenumber yields positive real and imaginary parts of the complex dynamic moduli. Also, the calculated transfer functions using equation (2) and the continuous set of these physically acceptable solutions of the wavenumber should be identical to the measured transfer function. Typically the measurements of dynamic properties of porous materials are performed in vacuum to minimize the effects from the interaction with the fluid - air. [6] The application of the method presented here allows one to measure dynamic properties in presence of air with minimum effects from the airborne wave propagation.

3. THE DAMPING OF STRUCTURES BY ACOUSTIC MATERIALS

In this section, damping of structural vibration is investigated. When granular materials are contained in cavities created by plates or beams, the vibration of the structure induces wave propagation as shown in Figure 3. In many cases the dimension of the granular material in the direction of the transverse vibration is much smaller than the lateral dimensions of the structure. Consequently, two-dimensional analysis of the wave propagation inside the granules can be applied. Pressure loading from the granular material to the structure is applied to the equation of motion of the structural vibration for acoustic-structure interaction analysis. A variational formulation, the Rayleigh-Ritz method, [19, 20] is used to analyze the vibration response after taking into accounts the acoustic-structure interaction. In the case of vibrating classical beams, the kinetic, T, and potential energy, V, for transverse vibration of the beam are calculated as:

$$V = \int_0^{L_b} \frac{1}{2} D\left(\frac{\partial^2 w}{\partial x^2}\right)^2 dx\,,\quad T = \int_0^{L_b} \frac{1}{2} M_b\left(\frac{\partial w}{\partial t}\right)^2 dx\,,\quad W = \int_0^{L_b} \frac{1}{2}\left[p_e(x,t) - p_g(x,t)\right] w(x,t)\,dx\,, \tag{3a,b,c}$$

where D is the bending stiffness, M_b is the mass per unit length of the beam, p_e is the external excitation and $p_g(x,t)$ is the pressure induced from vibration of the granular media per unit length. In the Rayleigh-Ritz method, the transverse displacement is approximated as

$$w(x,t) = \sum_{m=1}^{N} \phi_m(x)\alpha_m(t), \tag{4}$$

where ϕ_m are the trial functions chosen from a complete set, and α_m are the generalized coordinates. After substituting equation (4) into equation (3), Lagrange's equations of motion,

$$\frac{d}{dt}\left(\frac{\partial L_a}{\partial \dot{\alpha}_m}\right) - \frac{\partial L_a}{\partial \alpha_m} = 0, \qquad m = 1,2,...,N \tag{5}$$

are applied, where $L_a = T\text{-}V\text{+}W$ is the system Lagrangian. This yields a set of equations of motion

$$[M]\{\ddot{\alpha}\} + [K]\{\alpha\} = \{F\}, \tag{6}$$

where [M], [K] and {F} are the mass, stiffness and force matrices, respectively. The harmonic excitation of the beam is considered with the time dependence defined as $\alpha_{mn}(t) = \mathrm{Re}\{\hat{\alpha}_{mn} e^{i\omega t}\}$ to obtain the solution of equation (6). As a complete set of the trial functions, polynomial functions are used:

$$\phi_m(x) = x^m, m = 0, N\ . \tag{7}$$

To compute the pressure loading from the granular material, the frame wave component is considered after neglecting the airborne wave component. In this case, the equation of motion is given as [21]

$$\nabla^2 \mathrm{p} = \mathrm{c}^{-2}\frac{\partial^2 \mathrm{p}}{\partial \mathrm{t}^2}, \tag{8}$$

where p is the pressure induced by the frame wave component.

The general solution for the vibration of the granular material inside the cylindrical beam (Figure 3b) is (the periodicity of the vibrational modes in the θ-direction is used):

$$\hat{\mathrm{p}}(\mathrm{r},\theta,\omega) = \sum_{\mathrm{m}=1}^{\infty} \hat{\mathrm{A}}_{\mathrm{m}} \mathrm{J}_{\mathrm{m}}(\hat{\mathrm{k}}\mathrm{r})\cos(\mathrm{m}\theta + \gamma_{\mathrm{m}}), \tag{9}$$

where J_m is the m-th order Bessel functions. After obtaining the velocity potential[21], the velocity response of the medium is calculated. Consequently, the particle velocity in the radial direction is calculated as

$$\hat{\mathrm{v}}_{\mathrm{r}} = -(\mathrm{i}\omega\rho)^{-1}\sum_{\mathrm{m}=1}^{\infty} \hat{\mathrm{A}}_{\mathrm{m}}\hat{\mathrm{k}}\mathrm{J}'_{\mathrm{m}}(\hat{\mathrm{k}}\mathrm{r})\cos(\mathrm{m}\theta + \gamma_{\mathrm{m}}). \tag{10}$$

To calculate A_m and γ_{mn}, the boundary conditions are imposed from continuity of normal velocity at the boundaries as:

$$\hat{\mathrm{v}}_{\mathrm{r}}(\mathrm{r} = \mathrm{R},\theta,\omega) = (\mathrm{i}\omega)\hat{\mathrm{w}}(\mathrm{x},\omega)\cos\theta\ . \tag{11}$$

After determining the constants from the above boundary conditions, the acoustic pressure inside the circular beam is obtained. Finally, the pressure loading from the granular media to the structure is calculated as

$$\hat{p}_g(x,\omega) = -2\int_{-\pi/2}^{\pi/2} \hat{p}(r = R,\theta,\omega)\cos(\theta)R\,d\theta = -\pi R\rho_f \hat{c}_f \omega\, w(x,\omega)J_1(\hat{k}R)/J_1'(\hat{k}R). \tag{12}$$

From equation (6) and equation (12), the mass and stiffness matrices are calculated as

$$[M_{mp}] = \int_0^a M_b\phi_m(x)\phi_p(x)dx = \frac{M_b}{m+p+1}a^{m+p+1}, \tag{13a}$$

$$[K_{mp}] = \int_0^a D\frac{\partial^2\phi_m(x)}{\partial x^2}\frac{\partial^2\phi_p(x)}{\partial x^2} - \hat{K}_a\phi_m(x)\phi_p(x)dx = \begin{cases} -\dfrac{\hat{K}_a}{m+p+1}a^{m+p+1}, m < 2 \quad \text{or} \quad p < 2 \\ \dfrac{Dm(m-1)p(p-1)}{m+p-3}a^{m+p-3} - \dfrac{\hat{K}_a}{m+p+1}a^{m+p+1}, otherwise \end{cases} \tag{13b}$$

where $\hat{K}_a = \pi R\rho\hat{c}\omega\, J_1(\hat{k}R)/J_1'(\hat{k}R)$. The same numerical procedures can be applied to other structures containing damping treatment. In the case of a beam with rectangular cross-section, Figure 3a, the constant is calculated as $\hat{K}_a = 2h_w\rho\hat{c}\omega\,(1-\cos(\hat{k}h_t))/\sin(\hat{k}h_t)$, where h_w and h_t is the width and thickness of the beam, respectively.

After obtaining the mass and stiffness matrices in equation (13), the forced vibration response is calculated from the boundary conditions. Since the loading from the granular materials depends on the frequency, its impact on the forced vibration response also varies with frequency. Note from equation (13) that when the damping in the media is negligible (the wavenumber, $\hat{k}$, has only the real part) the

loading from the acoustic-structure interaction does not contribute to the damping of the structural vibration, although it has impact on the magnitude of the natural frequency. Only when the damping in the media is not negligible (the wavenumber has both of the real and imaginary parts), is the vibration damped due to the acoustic-structure interaction. This is especially evident at the natural frequencies where the dynamic impedance of the beam is small. The dissipation of the vibration energy through the lightweight granular material has the most significant impact on the loss factor of the bending stiffness when the damping in the structure itself is small. To estimate its impact on the structural vibration, the dynamic stiffness of the beam is obtained from both of the measured and calculated forced vibration response. The transfer function method for the classical beam[22] is used to calculate the dynamic stiffness. Consequently, the effects of the damping materials on the vibrating structure can be analyzed through the frequency dependence of the dynamic stiffness.

4. RESULTS AND DISCUSSIONS

A. Frame Vibration Characteristics

In the experimental setup to measure the frame wave characteristics, Figure 2, an electronic shaker (Brüel & Kjær type 4189) was used to induce the longitudinal excitation of the base panel. A random signal in the frequency ranging from 40 Hz to 2000 Hz was supplied to the shaker. A miniature piezoelectric accelerometer (Endevco model 2250-A) was attached to the center of the base panel to measure the input acceleration level, a_0 (= $-\omega^2 w_0$). The magnitude and phase of the acceleration measurements was calibrated with respect to the velocity measurement of a laser Doppler vibrometer that was used to measure the vibration of the attached mass. The transfer function between the two vibration measurements, w_0 and $w(x=h)$, was used to obtain the dynamic properties.

A wide range of specimens composed of different raw material and the particle diameters were tested – lightweight microspheres made of polyimide (Teek-L), glass spheres, fiberglass, and polyurethane acoustic foam. The densities and particle radii of the samples are shown in Table 1. For the glass spheres and microspheres, the particles were spherical. Each lightweight microsphere, particle includes a void in the center, and consequently the density varied with the particle radius. The thickness of the specimen, when testing the microspheres and glass spheres was 0.75 cm. For the fiberglass and the acoustic foam, it was 0.95 cm and 1.23 cm, respectively. Double-sided tape and spray epoxy were used on the base panel and the attached mass, respectively, when the acoustic foam and the fiberglass were tested.

Figure 4 shows the variation of the measured transfer functions with the input acceleration level for microspheres (R=190 μm) and acoustic foam– the input acceleration was imposed at x=0 (a_0). For the acoustic foam, the input and output response was coherent and there was little variation of the measured transfer functions with the input excitation level. This suggested that the linear longitudinal vibration analysis in section II was appropriate for use in the transfer function method. For the microspheres, there was considerable variation with the excitation level. The natural frequency and the peak amplitude decreased considerably with increasing vibration amplitude, which indicated that the damping inside the granular material increased with increasing vibration amplitude as also reported by Kuhl and Kaiser. [11]

The dynamic properties of the granular materials were calculated from the measured transfer functions. Figure 5 shows the frame wave speeds obtained for microspheres. The frame wave speed depended on the vibration amplitude and was much smaller than the airborne wave speed which ranges from 100 to 200 m/s for the microspheres. As expected from the measured transfer functions, the wave speeds decreased and the loss factor increased with increasing vibration amplitude. The dashed lines in Figure 5 are the values curve-fitted based on the measured values. Since the loss factor increases monotonically with frequency in the frequency range of interest, the loss factor was curve-fitted to the following approximate equation as

$$\eta_c = C_{1\eta_c} \log f + C_{2\eta_c} . \tag{14}$$

The measured loss factor increased in the frequency ranges of interest except for the frequencies where the coherence between the two vibration measurements was much less than one, i.e., when the assumption of simple longitudinal vibration of the specimen was not appropriate. The decay in the coherence had significant impact on the loss factor calculated after applying linear longitudinal vibration theories in the transfer function method. Consequently, the deviation of the calculated loss factor from the frequency dependence in equation (14) was more significant for larger vibration amplitude. At frequencies where the coherence was close to one, the measured loss factor increased following equation (14).

From the frequency dependence of the elastic modulus on the loss factor as $E(\omega) = E_d \omega^{\frac{2\eta_E}{\pi}}$ [18, 23], the frequency dependence of the wave speed was curve-fit to the following approximate equation:

$$c(\omega) = c_d \omega^{\frac{2\eta_c}{\pi}} . \quad (15)$$

The average of the loss factors in the frequency ranges that showed distinct frequency dependency as in equation (14) was used for the loss factor in equation (15). This frequency dependence shows that the dynamic stiffness of the material increases monotonically with increasing frequency. The degree of frequency dependence is determined by the loss factor. For a material with a large loss factor, the dynamic stiffness increases more rapidly with frequency than that with a smaller loss factor. [23]

The measured values of frame wave speed closely followed the frequency dependent relationship described by equation (15) as shown by the dashed lines in Figure 5. As the excitation level was increased, the loss factor increased, and consequently the degree of the frequency dependence of the wave speed was also increased. The frequency dependence shown in equation (15) is the typical characteristic of viscoelastic elastomers. [18,23] This suggests that the dynamic properties of the frame of the granular materials followed closely those of the viscoelastic materials. However the dynamic characteristics deviated from those of typical viscoelastic materials when the vibration amplitude was too large.

Similar analyses were repeated for the other porous and granular materials. Figure 6 shows the measured dynamic properties. Note that the sensitivity of the results to error in the measurement variables depends on the natural frequency of the measured transfer function and on the degree of the interaction of the frame waves with the acoustic wave propagation. The measured results are plotted in different frequency ranges in which the sensitivity was not significantly high. The wave speeds for the microspheres and the glass spheres were higher than those of the fiberglass and were lower than those of the acoustic foam. The loss factor of the fiberglass was much higher than the rest of the specimens for the excitation levels tested. The frequency dependence of the frame wave speed predicted by curve-fitted values using equation (15) (dashed lines) agreed well with the measured values for all specimens. Here too, the slope of the frame wave speed curve for porous and granular materials increases with increasing loss factor.

B. Vibration damping through porous materials

To investigate the damping of structures though the porous and granular materials, slip table tests [22] were performed for hollow aluminum cylindrical beams. The dimensions of the beams were o.d. 0.025 m, i.d. 0.022 m, and length (L_b) 0.9 m. One end of the beam was fixed to the slip table floor using an epoxy to impose the fixed-free boundary conditions. This was excited with an input beam acceleration level of 3.7 m/s^2. Figure 7 shows the measured and predicted transfer functions between the excitations at the fixed end of the beam (x=0) by the slip table and the beam response at x=L_b/3. Prediction is compared with measurement for two cases in which the beam cavity is either empty (undamped) or filled with microspheres, R=210 μm, (damped). The mass ratio of the microspheres to the beam was 5 %. This ratio decreases when lightweight microspheres of smaller density are used. The fundamental (first) natural frequency of the beam was 30 Hz. To predict the beam response, the Rayleigh-Ritz method for N=13 was used. For most of the results, the dynamic properties of the damping materials are given in the form of equations (14) and (15) whose coefficients are obtained from the measured values taken with an excitation of a_0=5.5 m/s^2. The exception was the polyurethane acoustic foams. For the acoustic foam, the wave speed was given as $\hat{c}$ =56(1+ 0.24 i) m/s in the Rayleigh-Ritz method. This was smaller than the measured values (≈ 80 m/s). The corresponding loss factor was larger than the measured value (≈0.12). This adjustment was required to take into account of the frictional contacts between the beam and the acoustic foam, although the foams were cut slightly larger than the i.d. of the beam and were tightly fitted to the beam without epoxy. In Figure 7, the discrepancies of the measured and predicted natural frequencies increased slightly with increasing frequency since the shear vibration of the beam is neglected in the classical beam theory. For both of the predictions and the measurements, the lightweight microspheres significantly reduced the vibration response of the beam at resonances.

Following the numerical procedures of the transfer function method for the classical beam [22], the dynamic stiffness and the loss factor was calculated from the measured and calculated transfer functions and is shown in Figure 8. Some discrepancies were observed for the beam damped by the microspheres, which were expected due to the amplitude-dependent frame characteristics and the dynamic range of the beam response. The dynamic range is more than 80 dB due to the modal response (Figure 8). Overall,

excellent agreement was obtained in predicting the frequency dependent variation of the bending loss factor. This suggests that the frame vibration of the porous materials in the cross-section of the beam increased the bending loss factor significantly. The maximum of the loss factor occurred when there was a resonance for the acoustic response of the frame along the cross-section, i.e., when $J_1'(\hat{k}R)$ is minimum. Figure 9 shows the analytical results to investigate the effects of dynamic properties on the bending loss factor by using the transfer function between the beam responses at x=0 and x=L_b/4. As the frame wave speed is decreased, the maximum of the bending loss factor occurred at lower frequencies (Figure 9a). The loss factor of the frame wave speeds had a strong effect on the magnitude of the bending loss factor at the maximum (Figure 9b). With increasing loss factor of the frame dynamic stiffness, the loss factor of the bending stiffness reduced in the peak amplitudes but showed broad characteristics.

5. CONCLUSIONS

In this study, experimental methods to measure the vibration characteristics of the frame for porous and granular materials were proposed, and the damping of structural vibration using porous and granular materials was considered. The measured dynamic properties followed the characteristics of typical viscoelastic materials: the dynamic moduli increased with frequency and its frequency dependence was determined by its loss factor. The bending stiffness of the cylindrical beams containing different damping materials was derived using the transfer function method from data acquired through the slip table tests. By using the measured frame properties of the damping materials, the loss factor of the beam was predicted. Comparison to measured values suggested that the acoustic-structure interaction between the frame of the damping material and the structure increased the vibration damping significantly. The maximum of the loss factor occurred at the first resonance frequency of the frame vibration in the cross section of the hollow beam. In future vibro-acoustic control applications, the measured properties of the vibration characteristics of granular and porous materials should be useful in understanding sound transmission characteristics.

References

1. D. Zenkert, An Introduction to Sandwich Construction (Chameleon Press Ltd., London, 1997).
2. M.A. Biot, “Theory of propagation of elastic waves in a fluid-saturated porous solid. I. Low-frequency range,” J. Acous. Soc. Am. 28, 168-191 (1956).
3. J.S. Bolton, N.M. Shiau, Y.J. Kang, “Sound transmission through multi-panel structures lined with elastic porous materials,” J. Sound Vib. 191, 317-347 (1996).
4. B.H. Song, J.S. Bolton, “A transfer-matrix approach for estimating the characteristic impedance and wave numbers of limp and rigid porous materials,” J. Acous. Soc. Am. 107, 1131-1152 (2000).
5. K. Khirnykh, A. Cummings, “The measurement of frame motion in flexible porous materials,” J. Acous. Soc. Am. 105, 755-761 (1999).
6. T. Pritz, “Frequency dependence of frame dynamic characteristics of mineral and glass wool materials,” J. Sound Vib. 106, 161-169 (1986).
7. D.L. Johnson and T.J. Plona, “Acoustic slow waves and the consolidation transition,” J. Acous. Soc. Am. 72, 556-565 (1982).
8. K. Attenborough, “Models for the acoustical properties of air-saturated granular media” Acta Acust. 1, 213-226 (1993)
9. J. F. Allard, M. Henry, J. Tizianel, L Kelders, W. Lauriks, “Sound propagation in air-saturated random packings of beads,” J. Acous. Soc. Am. 104, 2004-2007 (1998).
10. A. Cummings, H.J. Rice, R. Wilson, “Radiation damping in plates, induced by porous media,” J. Sound Vib. 221, 143-167 (1999).
11. W. Kuhl, H. Kaiser, “Absorption of structure-borne sound in building materials without and with sand-filled cavities,” Acustica 2, 179-188 (1962).
12. L. Cremer and M. Heckl 1988 Structure-Borne Sound. New York: Springer-Verlag.
13. J.M. Bourinet, D. Le Houédec “A dynamic stiffness analysis of damped tubes filled with granular materials,” Comput. Struct. 73, 395-406 (1999).
14. J. C. Sun, H. B. Sun, L. C. Chow, E. J. Richards, “Predictions of total loss factors of structures, Part II: Loss factors of sand-filled structure,” J. Sound Vib. 104, 243-257 (1986).
15. J. G. McDaniel and P. Dupont, “A wave approach to estimating frequency-dependent damping under transient loading,” J. Sound Vib. 231, 433-449 (2000).

16. ANSI S2.22-1998, “Resonance method for measuring the dynamic mechanical properties of viscoelastic materials,” American National Standards Institute, published through the Acoustical Society of America (New York, 1998)
17. T. –K. Ahn and K.-J. Kim, “Sensitivity analysis for estimation of complex modulus of viscoelastic materials by non-resonance method,” J. Sound Vib. 176, 543-561 (1994).
18. J. Park, T. Siegmund, and L. Mongeau, “Viscoelastic properties of foamed thermoplastic vulcanizates and their dependence on void fraction,” Cell. Polym. 22, 137-156 (2003).
19. L. Meirovitch Computational Methods in Structural Dynamics. (Sijthoff & Noordhoff, Rockville, Maryland, 1980)
20. A. Berry, “A new formulation for the vibrations and sound radiation of fluid-loaded plates with elastic boundary conditions” J. Acous. Soc. Am. 96, 889-901 (1994).
21. L.E. Kinsler, A.R. Frey, A.B. Coppens, and J.V. Sanders Fundamentals of Acoustics (John Wiley & Sons, Inc., New York, 1982)
22. J. Park “Transfer function methods to measure dynamic mechanical properties of honeycomb structures and beams,” submitted to Journal of Sound and Vibration.
23. T. Pritz, “Frequency dependences of complex moduli and complex Poisson’s ratio of real solid materials” J. Sound Vib. 214, 83-104 (1998).

Table 1. Mechanical properties of porous and granular materials under tests.

	Mean radius, R (μm)	Density (kg/m^3)
Microspheres (Polyimide-Teek – H)	300, 600	23, 23
Microspheres (Polyimide-Teek – L)	190, 210	49, 44
Glass spheres	33	1590
Polyurethan foam	.	37
Fiberglass	.	14

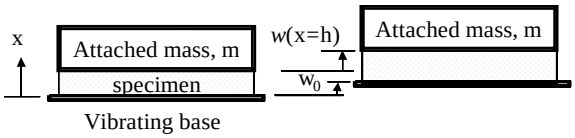

Figure 1. Longitudinal vibration of specimen.

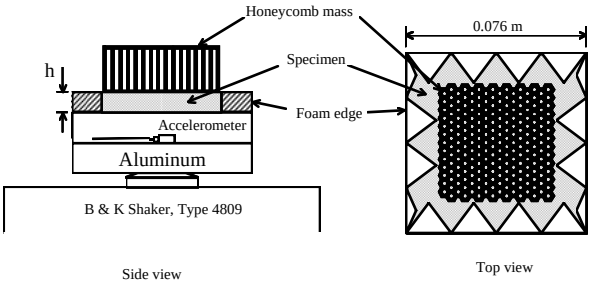

Figure 2. Experimental setup to measure frame dynamic properties of granular materials.

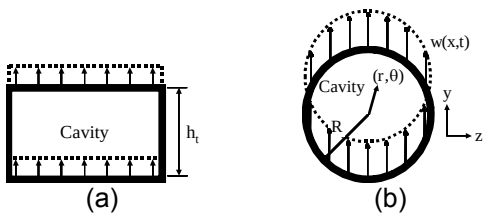

Figure 3. Vibration of damping materials induced by transverse bending vibrations of beams of (a) rectangular and (b) circular cross-sections.

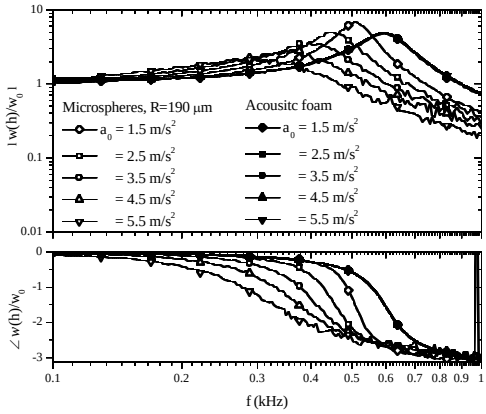

Figure 4. Measured transfer functions in case of microspheres (R=190 μm) and polyurethane acoustic foam.

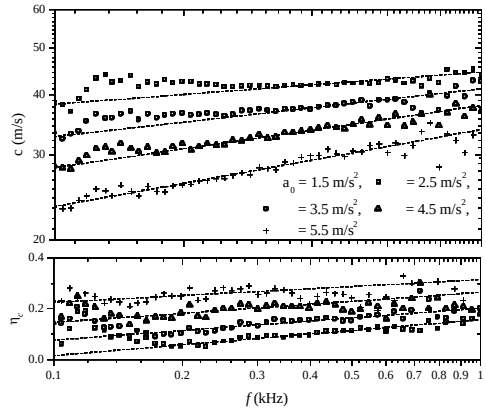

Figure 5. Effects of excitation amplitudes on the wave speed and its loss factor for microspheres of R=190 μm.

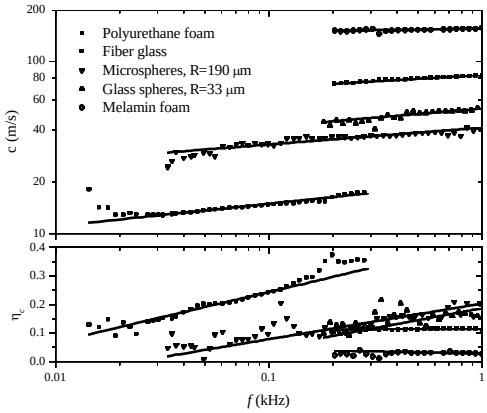

Figure 6. Wave speed and its loss factor measured for acoustic foam, fiberglass, microspheres, and glass spheres. a_0 = 3.5 m/s^2.

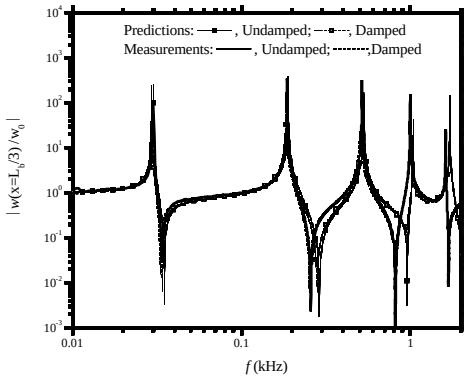

Figure 7. Transfer function for the vibration of the beam with (damped) and without (undamped) microspheres (R=210 μm) inside the beam cavity.

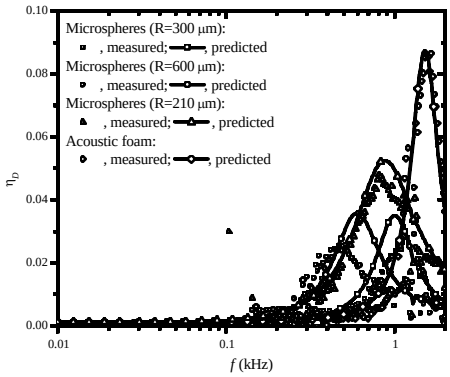

Figure 8. Measured and predicted loss factors of the bending stiffness when the beam is damped through microspheres and acoustic foam.

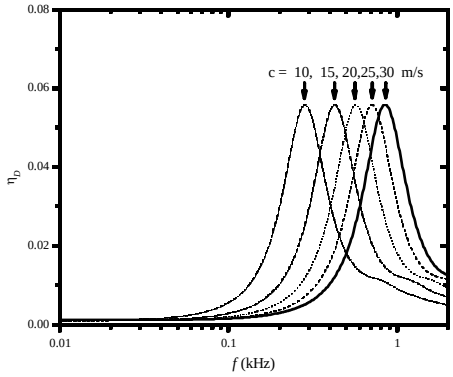

(a)

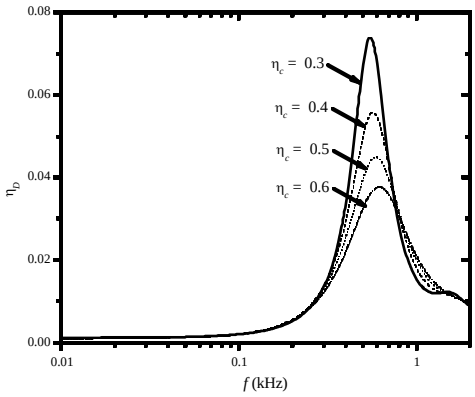

(b)

Figure 9. Variation of the loss factors of the beam bending stiffness with dynamic properties of microspheres. Effects of (a) frame wave speeds for η_c=0.4, and (b) its loss factors for c=20 m/s. ρ=40 kg/m^3.